Liquid-Liquid Phase Equilibria in Polymer Solutions and Polymer Mixtures

Attila R. Imre[1], W. Alexander Van Hook[2], Bernhard A. Wolf[3]*

[1] KFKI Atomic Energy Research Institute H-1525 Budapest, P.O. Box 49, Hungary
[2] University of Tennessee, Department of Chemistry, 37996 TN, Knoxville, USA
[2] Johannes Gutenberg Universität, Institut für Physikalische Chemie, Jakob-Welder Weg 13, D-55099 Mainz, Germany

Summary: The pressure dependence of liquid-liquid equilibria in weakly interacting binary macromolecular systems (homopolymer solutions and blends) will be discussed. The common origin of the separate high-temperature/low-temperature and high-pressure/low-pressure branches of demixing curves will be demonstrated by extending the study into the region of metastable liquid states including the undercooled, overheated and stretched states (i.e. states at negative pressures). The seemingly different response of the UCST-branch of solutions and blends when pressurized (pressure induced mixing for most polymer solutions, pressure induced demixing for most blends) will be explained in terms of the location of a hypercritical point found either at positive (most solutions) or negative pressure (most blends). Further, it is shown that the pressure dependence of demixing of homopolymer solutions and blends may be described using a ‚master-curve' which, however, is sometimes partly masked by degradation or by vapour-liquid and/or solid-liquid phase transitions. Experimental results demonstrating the extension of liquid-liquid phase boundary curves into the metastable regions will be presented, and the existence of solubility islands in the vicinity of the hypercritical points discussed.

Introduction

Weakly interacting binary homopolymer systems (polymer solutions and polymer blends) usually exhibit two-phase behaviour at low temperature, become homogeneous on increasing the temperature to intermediate values, and, finally, exhibit a second liquid-liquid phase transition at high temperature, where they may again split into two coexisting phases (Figure 1). For solutions and blends of this type two critical points are noted: the uppermost point of the low temperature branch (the Upper Critical Solution Temperature, UCST) and the lowest point of the high temperature branch (the Lower Critical Solution Temperature, LCST). Parts of the phase diagram (Figure 1) can be masked, for example should the freezing locus lie in the homogeneous region (no

 CCC 1022-1360/00/$ 17.50+.50/0

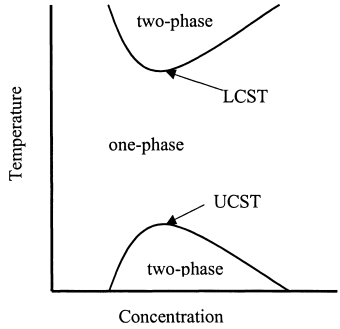

Figure 1. Liquid-liquid phase diagram for a binary homopolymer solution or blend (neglecting polydispersity effects).

UCST, only LCST), or by the thermal degradation of the polymer should LCST lie at extremely high T (no LCST, only UCST). The effects of pressure on the UCST and LCST of binary homopolymer solutions (polymer+solvent) and homopolymer blends (polymer+polymer) have been studied since the early sixties. Due to the wide variety of the L-L phase diagrams a general description of the effect of pressure is not easy. In Figure 2, several kinds of experimentally observed behaviours for UCST and LCST are schematically diagrammed in the (P,T) diagram.

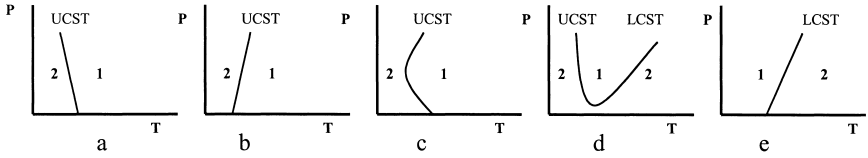

Figure 2. Commonly observed P-T dependencies of critical liquid-liquid loci of binary homopolymer blends and solutions.

The behaviour in Fig.2/a, $(dP/dT)_{UCST} < 0$ and approximately linear, is the one most often observed for solutions of polymers in small molecule solvents, and that in 2/b, $(dP/dT)_{UCST} > 0$ and linear, is commonly seen for polymer blends[1-4]. Fig. 2/a corresponds to the pressure induced miscibility (PIM) and 2/b corresponds to the pressure induced immiscibility (PII). Curved plots (Fig. 2/c) of UCST in the (P,T) projection have been reported for a number of polymer solutions (for example polystyrene/ methylcyclohexane[5-7]). Figure 2/d carries this forward to the case where both UCST and LCST curve markedly in the (P,T) projection and join at a hypercritical point. This behaviour is sometimes seen for solutions of polymers of high enough molecular weight in "poor" solvents (e.g. polystyrene/acetone, M_w>21 kg/mol)[8]. Finally, Figure 2/e shows the most commonly observed (P,T) dependence for solutions

or blends with only an LCST ($(dP/dT)_{LCST} > 0$ and approximately linear[9]). For many solutions both UCST and LCST branches are observed (e.g. polystyrene/cyclohexane), and sometimes (but far from always) these may join at a hypercritical point (Figure 2/d). In blends, however, most often only one branch is seen, either UCST (i.e. some blends of polyalkylsiloxanes[10]), or LCST (like polystyrene/poly(vinyl methyl ether[11]).

We propose that the various pressure dependencies discussed above are to be included in a common frame. It will be shown that the so-called Global Phase Diagram method[12], which is a system originally developed to describe fluid-fluid equilibria in small molecule mixtures, can also be applied to polymer/polymer and polymer/solvent mixtures. Furthermore, we claim the seemingly different behaviours of polymer solutions and polymer blends described above is caused by changes in the relative position of the two hypercritical points defining the particular solution or blend. An unusual phenomenon, the appearance of miscibility islands - also connected with the existence of hypercritical points – will be discussed.

General description

The different types of fluid-fluid (including liquid-liquid) phase equilibria in binary mixtures of small molecules can be characterised using the 'Global Phase Diagrams' (GPD) introduced by von Konynenburg and Scott[12]. Although GPDs were originally introduced to describe fluid-fluid equilibria in mixtures of van der Waals fluids, it has been shown recently[3,4,13] that the 'so-called' Type IV. and Type III. diagrams also represent liquid-liquid equilibria in polymer solutions and blends (Figure 3).

In the Type III. diagram three extrema (often called hypercritical points) can be seen, namely the Critical Temperature Minimum (CTM), the Critical Pressure Minimum (CPMin) and the Critical Pressure Maximum (CPMax). For Type IV. only two extrema are shown (CTM and CPMax), the third has apparently been depressed into the (P,T/-,+)

quadrant. In support of this interpretation we point out that it has been known for decades that liquid-liquid phase equilibrium curves can be extended into regions where liquids became metastable so far as liquid-vapour and/or liquid-solid phase transitions are concerned (i.e. into the (P,T) region which, in the first case, lies below the vapour pressure curve, or in the second, below the freezing point line)[14-15]. So far as the L-L demixing locus is concerned, the only difference between Type III. and Type IV. Diagrams is that in Type IV. the bottom of the L-L locus (i.e. CPMin) has shifted below

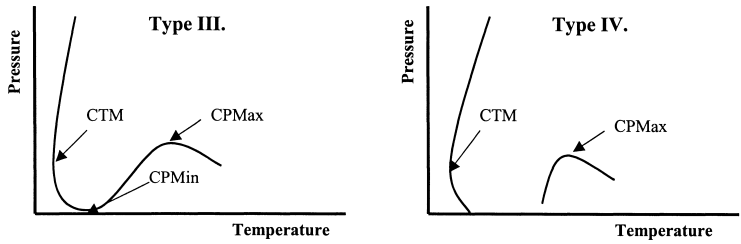

Figure 3. Liquid-liquid (P,T) demixing loci of Type III. and Type IV. mixtures (using the classification of von Konynenburg and Scott [12]). CTM: Critical Temperature Minimum, CPMin: Critical Pressure Minimum, CPMax: Critical Pressure Maximum.

the vapour pressure curve, and perhaps even below zero pressure[16,17]. CPMin still exists but is masked by the boiling curve. Similarly, in certain cases CTM, even though it may lie at conveniently accessible P, may be masked by the freezing locus of the solution, which, in turn, is determined by solvent properties and/or polymer M_w. Even so, it follows that a master curve similar to Type III. should describe L-L loci of present interest (Figure 4), although parts of the master curve for certain solutions may lie in metastable and/or experimentally inaccessible parts of the phase diagram.

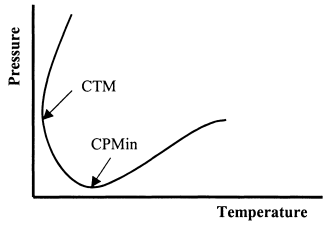

Figure 4. General pressure dependence of the liquid-liquid locus in polymer solutions and polymer blends.

In Figure 4 note that at high temperature the (P,T) demixing locus, while tending to CPMax (see Fig. 3), does not actually display that maximum. While theoretically possible, to our knowledge such a maximum has never been seen in polymer solutions or blends. In those small molecule systems where CPMax has been observed, it typically

lies well above the vapour-liquid critical curve of the more volatile component. For polymer solutions, the more volatile component is the solvent, and for most organic solvents the V-L critical temperature lies well above 200 Celsius, where the polymer is likely thermally degraded. Thus, it is unlikely that CPMax can be reached experimentally, but the high temperature part of the locus, above CPMin, can be found

in simulations[18,19]. In polymer blends CPMax will be located at even higher temperature than for solutions, and only the lower and nearly linear part of the LCST curve is experimentally observed. Depending on the location of the other two extrema, CTM and CPMin, different (P,T) behaviours are observed for UCST and LCST. For most polymer blends, CPMin lies below P=0, but CTM may or may not be below P=0. Therefore, depending on the freezing points of the compounds, one expects only UCST with $(dP/dT)_{UCST} > 0$ [2], or only LCST with $(dP/dT)_{UCST} > 0$. In a few blends, CTM is found above P=0 (see [20] and references therein], and in these systems UCST behaviour with $(dP/dT)_{UCST} < 0$ is observed. Most often, CTM is located above the experimentally accessible P, but in a few cases UCST curves markedly in the (P,T) plane and CTM is observed[21-23]. Using oligostyrene/oligoethylene as a model system, it was recently shown for blends containing short chain polymers CTM lies above P=0, but with increasing chain length CTM falls to lower pressure and finally "disappears" below the vapour pressure curve[20,24] (Figure 5).

For polymer solutions, UCST systems with $(dP/dT)_{UCST}<0$ and LCST with $(dP/dT)_{LCST}>0$ are the most common (see references of [3,4]). In some solutions (like polystyrene/cyclohexane[25]) $(dP/dT)_{UCST}$ changes sign at a certain molecular weight; similar effect has been predicted for some blends[26]. Using the interpretation above it is

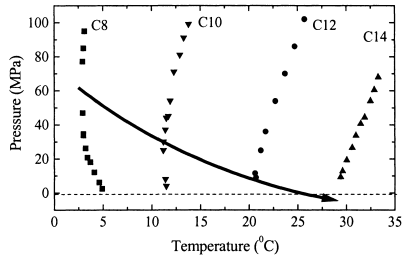

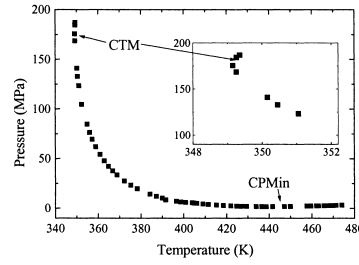

Figure 5. (left) Pressure dependence of the UCST of oligostyrene/oligoethylene (n-alkane) mixtures. The chain length dependence of CTM is shown as the heavy arrow[20]. Linear n-alkanes have been used as models for oligoethylenes, C8: n-octane, C10: n-decane, C12: n-dodecane and C14: n-tetradecane, M_w^{PS}=1.2 kg/mol.

Figure 6. (right) Pressure dependence of the liquid-liquid locus in a polystyrene/trans-1,4-dimethylcyclohexane solution (M_w=575 kg/mol, M_w/M_n=1.07, polymer concentration=7 w%) exhibiting two hypercritical points, CTM and CPMin.

easy to recognize such behaviour is due to the chain length dependence of CTM.

In some polymer/poor-solvent solutions the UCST and LCST branches join at a hypercritical point provided M_w is above some limiting value. Below that critical M_w the solutions exhibit separate UCST and LCST branches with $(dP/dT)_{UCST} < 0$ and $(dP/dT)_{LCST} > 0$. It has been shown experimentally, that the virtually separated UCST and LCST branches continue into the metastable regions (metastable for liquid-vapour phase transition) below the vapour pressure curve, and even below P=0, where they join at a metastable hypercritical point[16,17].

Polymer solutions exhibiting both CTM and CPMin at experimentally accessible P and T have been recently reported[3,4] (Figure 6) and the observation used to support the argument that the Type III. 'master' diagram can be used for the general description of the liquid-liquid demixing of polymer solutions and blends.

Solubility Islands

It is well understood that the polydispersity of polymers accounts (at least in most cases) for the fact that the coexistence and cloud point curves (CPCs) which describe liquid-liquid demixing do not coincide in polymer solutions and blends (except at the critical concentration). The quantitative description of the differences between the coexistence and CPC, which may be considerable, depends sensitively on the molecular weight distribution[8,27]. In demixing it is the CPCs which are most commonly measured; typically, on cooling one marks that T where the initially clear solution turns 'cloudy', due to the appearance of droplets of the second-phase. In a monodisperse polymer solution (or blend) the UCST lies at the top of CPC in the (ϕ,T) diagram (ϕ = concentration); but for polydisperse solutions UCST moves to the high concentration side of the maximum in CPC. Koningsveld and coworkers have pointed out that polydisperse blends or solutions sometimes display double humped CPCs with the UCST sitting in the local minimum, and this effect of polydispersity may account for solubility islands (one-phase islands placed inside of the two-phase regions) in the (ϕ,T) projection[28,29,30]. The present approach which employs arguments based on Global Phase Diagrams (vide supra) generalizes and extends such ideas to (ϕ,P) space. One can easily see that in both the (ϕ,P) and (ϕ,T) projections the combination of such a double humped concentration dependence for CPC with the general (P,T) dependence described by a Type III. master diagram containing CTM and CPMin (Figure 3) leads to

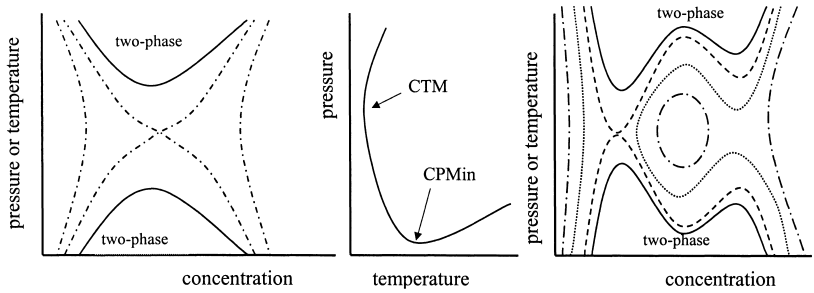

Figure 7. The formation of a solubility island. In the middle (7/b), a liquid-liquid locus can be seen exhibiting CTM and CPMin. On approaching CTM or CPMin by decreasing the temperature or pressure, the separated branches (for CTM: the high-pressure and low-pressure branches in (ϕ,P) space, for CPMin: the high-temperature (LCST) and low-temperature (UCST) branches in (ϕ,T) space) will merge. In case of single humped cloud point curves, an hour-glass type two-phase region will form (Figure 7/a, left), but for double humped CPCs first a solubility peninsula, then a solubility island, will form inside the hour-glass type two-phase region (Figure 7/c, right). The dotted, dashed, dash-dotted and solid lines in figures 7/left and 7/right represent constant temperature or pressure cuts.

the prediction of solubility islands in the (ϕ,T) and/or (ϕ,P) cuts (Figure 7). In fact, the existence of solubility islands in (ϕ,T) space was first predicted in the early nineties[31] and experimentally observed a few years later[8,32], but in the (ϕ,P) domain the solubility island was found prior to any prediction[24,33]. (In this context it is necessary to mention the well known existence of miscibility islands in (ϕ,T) and (ϕ,P) space, the islands being two-phase regions surrounded by a one-phase region[15], but this kind of behaviour does not occur in weakly interacting binary systems.)

The formation of solubility islands is qualitatively outlined in Figure 7. In the monodisperse case (Figure 7/left), one approaches the hypercritical points (decreasing P when nearing CPMin, or decreasing T when nearing CTM). This causes the two branches to merge (toward high temperature and low temperature, respectively, during the approach to CPMin, or toward high pressure and low pressure on the approach to CTM). In the monodisperse case, the two branches merge to yield an hour-glass type two-phase region with polymer-rich and polymer-poor coexisting solutions confined to rather small and rather high concentrations. The merging of the upper and lower two

phase regions takes place in an entirely different fashion for systems with double-humped CPCs (Figure 7/right). The two branches join first at the maximum and minimum of the more prominent humps, forming a solubility peninsula, then secondly, join at the smaller humps, to forming the hour-glass type two-phase region already seen in monodisperse systems but now with an extra solubility island (a one-phase island placed inside of the two-phase region). As one further continues the approach to one or the other hypercritical point, CPmin or CTM, the solubility island shrinks and finally disappears. Thus, two conditions are necessary to generate a solubility island. First, there must be an accessible (or nearly accessible) hypercritical point (CTM or CPMin). Second, CPC must be double humped in (ϕ,T) space to generate an island around CPMin, or double humped in (ϕ,P) space to yield an island about CTM.

The existence of solubility islands (especially the one around CTM, which is located at lower temperature, i.e. probably below any degradation temperature) might give us a new (and hopefully practical) way to homogenise virtually incompatible polymers. For nearly incompatible polymers one finds CPC's like that in Figure 8/left. Blends can be prepared only at very small or very high concentration. For recycling, however, it is advantageous to prepare homogeneous mixtures at more or less equal concentrations of the two polymers. With one or more solubility islands somewhere in the (ϕ,T,P)

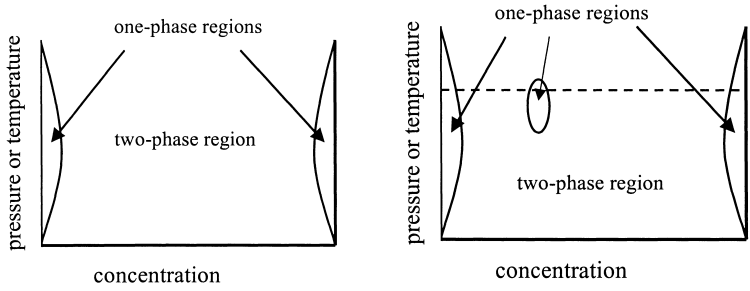

Figure 8. (left): Cloud point curves of two 'incompatible' polymers showing a large hour-glass type two phase region and with two small one-phase regions located at very low and very high concentrations, (right): Cloud point curves of two 'virtually incompatible' polymers showing a large hour-glass type two-phase region and three smaller one-phase regions, two located at very low and very high concentration, and the third one (an island), found inside of the two-phase region (not necessarily in the middle).

processing space of interest (Figure 8/right), it might be possible to generate a homogeneous mixture, then quench to a solid one-phase (metastable) material for use in further processing. Although CTM for blends is usually located below P=0, the topmost part of the island might reach the experimentally more accessible $P>P_{vap}$ region (above the dashed line on Figure 8/left).

Conclusions

A general phase diagram has been introduced to describe the pressure dependence of liquid-liquid phase equilibria in weakly interacting binary homopolymer blends and solutions. Experimentally observed differences in pressure induced behaviours are due to the relative positions of two hypercritical points, CTM and CPMin, on a master demixing curve. For samples with double humped cloud point curves, one predicts the presence of solubility islands lying well inside the two-phase regions. In favourable cases one or both hypercritical points (and the corresponding islands) might be experimentally accessible, thereby yielding a new tool to homogenise virtually incompatible polymers.

Acknowledgement

This work was partially supported by the Hungarian Science Foundation (OTKA), by the U.S. Department of Energy and by the Humboldt-Foundation (Germany). A.R.I. was also supported by the Bolyai Research Fellowship.

[1] B.A. Wolf, H. Geerisen, *Colloid. Polym. Sci.* **1981**, *259*, 1214.
[2] M. Rabeony, D.J. Lohse, R.T. Garner, S.J. Han, W.W. Graessley, K.B. Migler, *Macromolecules* **1998**, *31*, 6511.
[3] A.R. Imre, G. Melnichenko, W.A. Van Hook, *Phys. Chem. Chem. Phys.* **1999**, *1*, 4287.
[4] A.R. Imre, G. Melnichenko, W.A. Van Hook, *J. Polym. Sci. B.* **1999**, *37*, 2747.
[5] S. Vanhee, F. Kiepen, D. Brinkmann, W. Borchard, R. Koningsveld, H. Berghmans, *Macromol. Chem. Phys.* **1994**, *195*, 759.
[6] H. Hosokawa, M. Nakata, T. Dobashi, *J. Chem. Phys.* **1993**, *98*, 10078.
[7] P.A. Wells, Th.W.de Loos, L.A. Kleintjens, *Fluid Phase Equilib.* **1993**, *83*, 383.
[8] M. Luszczyk, L.P.N. Rebelo, W.A. Van Hook, *Macromolecules* **1995**, *28*, 745.
[9] I.H. Kim, J.G. Jang, Y.C. Bae, *Polymer* **1998**, *39*, 6905.
[10] A. Stammer, B.A. Wolf, *Polymer* **1998**, *39*, 2065.
[11] T. Nishi, T.T. Wang, T.K. Kwei, *Macromolecules* **1975**, *8*, 227.
[12] P.H. von Konynenburg, R.L. Scott, *Phil. Trans. Roy. Soc.* **1980**, *298*, 495.
[13] L.V. Yelash, T. Kraska, *Phys. Chem. Chem. Phys.* **1999**, *1*, 4315.
[14] J. Timmermans, J. Lewin, *Discuss. Faraday Soc.* **1953**, *15*, 197.
[15] G. M. Schneider, *Ber. Bunsen Ges.* **1972**, *76*, 325.
[16] A. Imre, W.A. Van Hook, *J. Polym. Sci. B.* **1994**, *32*, 2283.
[17] A. Imre, W.A. Van Hook, *Chem. Soc. Rev.* **1998**, *27*, 117.

[18] G. Luna-Barcenas, J.C. Meredith, I.C. Sanches, K.P. Johnston, D.G. Gromov, J.J. de Pablo, *J. Chem. Phys*. **1997**, *107*, 10782.
[19] S. Saeki, *Fluid. Phase. Equilib*. **1997**, *136*, 87.
[20] A.R. Imre, G. Melnichenko, W.A. Van Hook, B.A. Wolf, *Phys. Chem. Chem. Phys*. **2001**, *3*, 1063.
[21] B. Rudolf, H.-J. Cantow, *Macromolecules* **1995**, *28*, 6595.
[22] D. Schwahn, *Macromol. Symp*. **2000**, *149*, 43.
[23] D. Schwahn, H. Freilinghaus, K. Mortensen, K. Almdal, *Macromolecules* **2001**, *34*, 1964.
[24] A.R. Imre, T. Kraska, L.V. Yelash, *Phys. Chem. Chem. Phys*. (accepted).
[25] S. Saeki, N. Kuwahara, M. Nakata, M. Kaneko, *Polymer* **1975**, *16*, 445.
[26] I.G. Economou, *Macromolecules* **2000**, *33*, 4954.
[27] M. Luszczyk, W. A. Van Hook, *Macromolecules* **1996,** *29*, 6612.
[28] R. Koningsveld, M.H. Onclin, L.A. Kleintjens in: "*Polymer compatibility and incompatibility, Principles and Practices"*, MMI Press Symposium Series, vol.2, (Ed.: K. Solc), Harwood Academic Publisher, Chur 1982.
[29] K. Solc, W. H. Stockmayer, J. E. G. Lipson, R. Koningsveld in: "*Multiphase Macromolecular Systems"*, B. M. Culbertson, Ed. Plenum Publishing Corp., New York 1989.
[30] S. Vanhee, R. Koningsveld, H. Berghmans, *J. Polym. Sci. B*. **1994**, *32*, 2307.
[31] C. Qian, S.J. Mumby, B.E. Eichinger, *J. Polym. Sci. B*. **1991**, *29*, 635.
[32] L. P. Rebelo, W. A. Van Hook, *J. Polym. Sci. B*. **1993**, *31*, 895.
[33] A.R. Imre, *J. Polym. Sci. B*. (submitted).